MNK Publication

International Journal of Latest Research in Science and Technology **ISSN (Online):2278-5299**
Volume 4, Issue 2: Page No.26-30, March-April 2015
https://www.mnkpublication.com/journal/ijlrst/index.php

QUANTUM DOTS SOLAR CELLS BASED ON CdS/CdSe/ZnS-TiO_2 PHOTOANODES

H. T. Tung*[1], N. T. Nguyen[1]
[1]Faculty of Physics, Dong Thap University, Dong Thap Province, Vietnam
*For Correspondence: E-mail:tunghtvlcrdt@gmail.com

Abstract:- In this work, we conducted the photovoltaic based on a set of CdS/CdSe/ZnS photo anodes by using successive ionic layer adsorption and reaction (SILAR) processes. The results show that the open circuit increased from 0.29 V to 0.79 V because the excited electrons were efficiently generated in the conduction band of quantum dots when the number SILAR changed. Furthermore, the effect of SILAR cycles on the recombination resistance was discussed to base on the electrochemical impedance spectroscopy results.

Keywords: Quantum dots, Solar cells, SILAR.

I. INTRODUCTION

Quantum dot-sensitized solar cells (QDSSCs) are considered as a promising low-cost alternative for third generation photovoltaic (Grätzel, 2001). This solar cell is sourcing from the dye-sensitized solar cell (DSSC), which is based on sandwich dye-sensitized nano crystalline work electrode, counter-electrode and electrolyte. Compared to the conventional DSSC, the sensitizer of QDSSC is replaced by semiconductor quantum dots (QDs) such as CdS (Wijayantha et al.., 2004), PbS (Lee et al.., 2009), Ag_2S (Tubtimtae et al.., 2010), CdSe (Fuke et al.., 2010), Ag_2Se (Tubtimtae et al .., 2011), CdTe (Bang et al.., 2009) and InAs (Yu et al.., 2006) which possess multiple advantages as tunable band gaps, high extinction coefficient, and high photo stability (Gorer et al.., 1994; Moreels et al.., 2007; Nozik et al.., 2008). Unfortunately, QDSSC which promises a high theoretical efficiency up to 44% for its special multi electrons generation character (Hanna et al.., 2006), still presents lower energy conversion efficiency and far below the theoretical value. For QD-sensitizers, CdS, CdSe and ZnS have been paid much attention because of their high potential in photo absorption under visible region. The two materials exhibit different characteristics. For CdS, its conduction band (CB) edge is higher than that of TiO_2, making the electron injection from CdS to TiO_2 very effective, but the absorption range of CdS is too narrow, which restrict the utilization of light. Lee (Lee et al.., 2009) model system prepared by successive ionic layer adsorption and reaction (SILAR) process is favorable than single CdS or CdSe, which is due to the extension of spectral response in the visible light region and charge injection from QDs to TiO_2. The influence of SILAR cycles on the device performance has also been investigated recently (Gonzalez-Pedro et al.., 2010). However, the detailed optical and especially electrochemical properties of the photo anodes with different SILAR cycles are still lack of deep research.

In this paper, we conducted CdS/CdSe/ZnS co-sensitizer on meso porous TiO_2 surfaces with different SILAR cycles. The optical properties of the photo anodes and the photovoltaic performance of the corresponding solar cells were investigated. Moreover, electrochemical impedance spectroscopy (EIS) was employed to investigate the interface impedance and chemical capacitance of the cells. Based on the EIS results, the SILAR deposition cycles effect on the charge recombination was discussed.

II. EXPERIMENT

Materials. $Cd(CH_3COO)_2.2H_2O$ (99%), KCl, Na_2S, $Zn(NO_3)_2$, Se powder, S powder, Na_2SO_3, $TiCl_4$, TiO_2 paste obtained from Dyesol, Australia.

Preparation on TiO_2 films, the TiO_2 thin films were fabricated by silk-screen printing with commercial TiO_2 paste. Their sizes ranged from 10 to 20 nm. Two layes of film with thickness of 8 µm (measured by microscope). Then, the TiO_2 film was heated at 400°C for 5 min and 500°C for 30 min. Afterward, the film was dipped in 40-mmol $TiCl_4$ solution for 30 min at 70°C and heated at 500°C for 30 min. The specific surface area of the mesoporous TiO_2 were investigated by using the N_2 adsorption and desorption isotherms before and after the calcination. The surface area is 120.6 m^2g^{-1}(measured by BET devices). This result indicates that the synthesized material has wider mesoporous structure.

Preparation on TiO_2/CdS/CdSe/ZnS films, the highly ordered TiO_2 were sequentially sensitized with CdS, CdSe and ZnS QDs by SILAR method. First, the TiO_2 film was dipped in 0.5 mol/L $Cd(CH_3COO)_2$-ethanol solution for 5 min, rinsed with ethanol, dipped for 5 min in 0.5 mol/L Na_2S-methanol solution and then rinsed with methanol. The two-step dipping procedure corresponded to one SILAR cycle and the incorporated amount of CdS QDs was increased by repeating the assembly cycles for a total of three cycles. For the subsequent SILAR process of CdSe QDs, aqueous Se solution was prepared by mixing Se powder and Na_2SO_3 in 50ml pure water, after adding 1 mol/L NaOH at 70◦C for 7h. The TiO_2/CdS samples were dipped into 0.5 mol/L $Cd(CH_3COO)_2$-ethanol solution for 5 min at room

Publication History
Manuscript Received : *21 March 2015*
Manuscript Accepted : *2 April 2015*
Revision Received : *24 April 2015*
Manuscript Published : *30 April 2015*

temperature, rinsed with ethanol, dipped in aqueous Se solution for 5 min at 50◦C, rinsed with pure water. The two-step dipping procedure corresponds to one SILAR cycle. Repeating the SILAR cycle increases the amount of CdSe QDs (a total of four cycles). The SILAR method was also used to deposit the ZnS passivation layer. The TiO_2/CdS/CdSe samples were coated with ZnS by alternately dipping the samples in 0.1 mol/L $Zn(NO_3)_2$ and 0.1 mol/L Na_2S-solutions for 5 min/dip, rinsing with pure water between dips (a total of two cycles). Finally, it was heated in a vacuum environment with different temperatures to avoid oxidation (see Fig. 1). The TiO_2/CdS/CdSe/ZnS was measured thickness by microscopic. The results of the average thickness of CdS (1), CdSe (1), ZnS (1) are 40nm, 43.3nm, 40nm respectively.

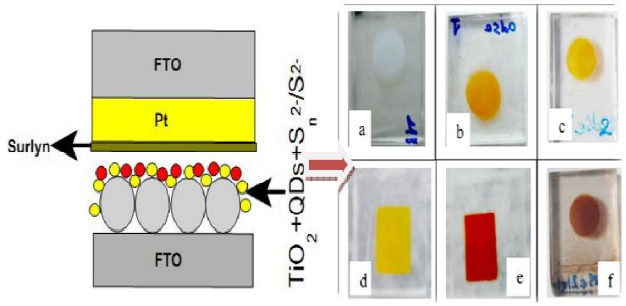

Figure 1. The diagram shows the instruction of the QDSSCs

Fabrication on QDSSCs: The polysulfide electrolyte used in this work was prepared freshly by dissolving 0.5 M Na_2S, 0.2 M S, and 0.2 M KCl in Milli-Q ultrapure water/methanol (7:3 by volume). The CdS/CdSe/ZnS co-sensitized TiO_2 photoanode and Pt counter electrode were assembled into a sandwich cell by heating with a Surlyn. The electrolyte was filled from a hole made on the counter electrode, which was later sealed by thermal adhesive film and a cover glass. The active area of QDSSC was 0.38 cm^2.

Characterizations and measurements

The morphology of the prepared samples was observed by using field-emission scanning electron microscopy (FE-SEM, S4800). The crystal structure was analyzed with an X-ray diffractometer (Philips, Panalytical X'pert, CuKα radiation). The absorption properties of the samples were investigated using a diffuse reflectance UV–vis spectrometer (JASCO V-670). Photocurrent – Voltage measurements were performed on a Keithley 2400 sourcemeter using a simulated AM 1.5 sunlight with an output power of 100 mW/cm^2 produced by a solar simulator (Solarena, Sweden).

III. RESULTS AND DISCUSSION

Figure2 shows the UV–Vis of different photoanodes measured after each cycle of SILAR. As result as, the intensity of absorbance spectra increased with the deposited cycles of CdS, CdSe and ZnS. So, only absorption spectra with SILAR cycles of the TiO_2/CdS(3)/CdSe(3)/ZnS(2) photoanode shows the best photovoltaic performance as discussed in the following section.

In short-wavelength region (380–550 nm), the increase of absorbance is due to more CdS was loaded on TiO_2 film and the co-absorption of CdS, CdSe and ZnS. In long-wavelength region (550–629 nm), the deposition of higher amounts of CdSe and ZnS on TiO_2/CdS electrode results in the increase of absorbance.

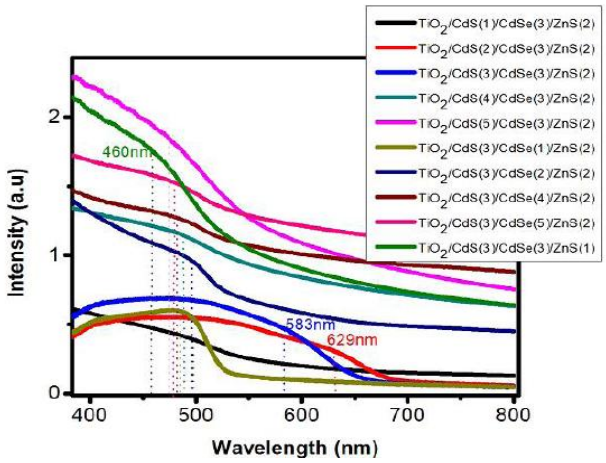

Figure 2. Absorption spectra of different TiO_2/CdS/CdSe/ZnS photoanodes

Moreover, the increasing successive deposition cycles also triggers a red shift of absorption spectrum which is due to a slight loss of quantum confinement effect (Pathan et al.., 2004). The evaluated sizes of CdS, CdSe and ZnS are consistent with the sizes measured from the FE-SEM images. The effect of deposition cycles of CdS, CdSe and ZnS can be clearly seen on the energy band gap values of CdS/CdSe/ZnS co-sensitized TiO_2 films. The estimated band gaps vary from 1.97 eV to 2.7 eV, which are higher than the values reported for CdS and CdSe in bulk (2.25 eV and 1.7 eV (Grätzel, 2001), respectively), indicating that the sizes of CdS, CdSe and ZnS on TiO_2 films are still within the scale of QDs. A higher absorption is thus obtained because the absorption spectrum of ZnS complements those of the CdSe and CdS QDs. Furthermore, ZnS acts as a passivation layer to protect the CdS and CdSe QDs from photo corrosion (Tachan et al.., 2011).

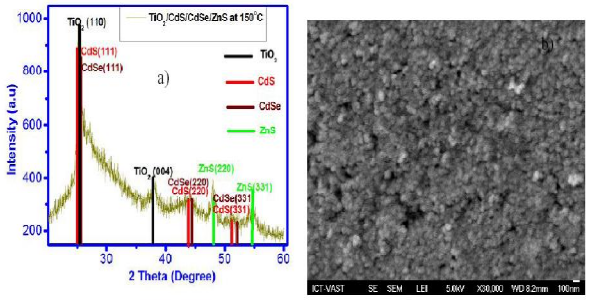

Figure 3.a) XRD and FESEM of CdS/CdSe/ZnS-TiO_2photoanodes.

The structure of the TiO_2/QDs photo electrodes for photovoltaic applications, shown in Fig. 3(a), are studied by the XRD patterns. It reveals that the TiO_2 have a anatase structure with a strong (101) peak located at 25.4º, which indicates that the TiO_2 film are well crystallized and grow along the [101] direction. Three peaks can be observed at

26.4º, 44º and 51.6º, which can be indexed to (111), (220) and (331) of cubic CdS, CdSe respectively. Two peaks can be observed at 48º and 54.6º, which can be indexed to (220) and (331) of cubic ZnS respectively. It demonstrates that the QDs have crystallized onto the TiO_2 film From FE-SEM at Figure 3b, we shows that the photo anode is high porous with the mean size about 20 nm. Due to between TiO_2 nanoparticles have a lot of space, so the CdS QDs is easy loaded on the TiO_2 nanoparticles.

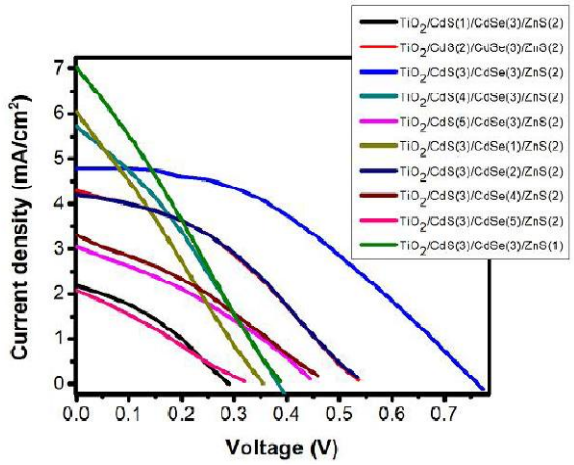

Figure4. The J–V curves of the QDSSCs with different photoanodes under one sun illumination.

In order to understand the effects of SILAR cycles of CdS, CdSe and ZnS, we prepared a set of combinedCdS, CdSe and ZnS QDs on TiO_2 films, investigated their photovoltaic performances with polysulfide electrolyte. All the samples were coated with ZnS to inhibit the recombination at the TiO_2 photo anode/polysulfide electrolyte interface (Lee et al.., 2009). Fig. 4 presents the photocurrent density voltage characteristics of the QDSSCs with different CdS/CdSe/ZnS co-sensitized TiO_2 films (active area of 0.38 cm^2) at AM 1.5 (100 mW/cm^2), and the related parameters of these QDSSCs are shown in Fig 5. Fig. 4 shows that the power conversion efficiencies of QDSSCs are increasing with the SILAR cycle number of CdS, CdSe and ZnS at 3, 3 and 2, respectively. It is noted that lower power conversion efficiency was obtained for those cells with either less CdS and CdSe SILAR cycles than 3 or more CdS and CdSe SILAR cycles than 3. The TiO_2/CdS(3)/CdSe(3)/ZnS(2) device shows an open-circuit voltage (V_{oc}) of 0.76 V, a short-circuit current density (J_{sc}) of 4.79 mA/cm^2, fill factor (FF) of 0.41 and an energy conversion efficiency (**η**) of 1.52%. When the deposition cycles of CdS and CdSe increase, slightly changes in V_{oc} and FF values were obtained. Remarkably, the J_{sc} decreases, which result in a substantial reduce of **η** (from 1.52% to 0.45%). These results indicate that although better light absorption performance were obtained when more CdSe loaded on TiO_2/CdS, the excessive CdSe on TiO_2/CdS films may lead to an increase of recombination in photo anodes. On the contrary, the increase of ZnS leads to the increasing generation of photoelectron and is helpful to collect excited electrons from ZnS, CdSe and CdS to TiO_2 film.

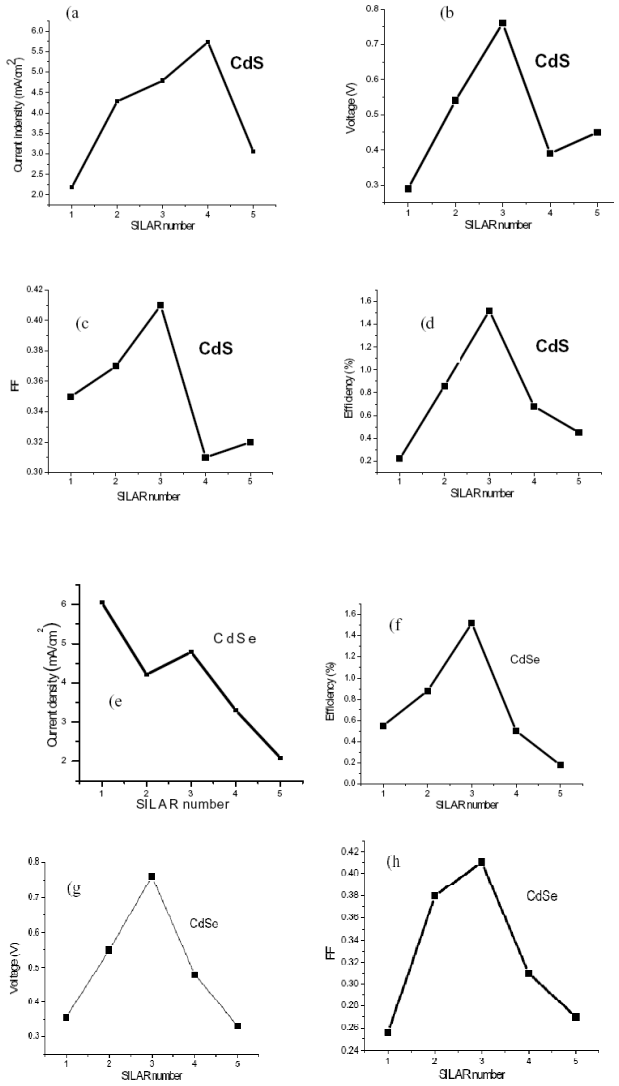

Figure 5. Diagrams show the changed parameters which depend on SILAR number of CdS and CdSe

The TiO_2/CdS/Cdse/ZnS co-sensitized solar cells demonstrated a better performance (1.52%) than the TiO_2/CdS (0.92%) and TiO_2/CdSe QDSSC (0.31%) (Chang et al.., 2009). This suggests that the charge injection from the conduction level of QDs to the conduction level TiO_2 may be effective, due to the quasi Fermi levels of QDs being longer than that of TiO_2(Lee et al.., 2009). Moreover, A ZnS coating forms a potential barrier between the QDs and the electrolyte, which blocks the electrons in the CB of QDs from recombination with the electrolyte (Sudhagar et al.., 2009). Resulting in a high performance of efficiency. From figure 5, it is evident that the photocurrent density of the coupled QDSSC was influenced by CdS/CdSe/ZnS co-sensitization cycles (Balisa et al .., 2013), which can be explained in two ways. First, size ofCdS, CdSe and ZnS QDs decreased due to results in cascade energy level structure in the order of TiO_2<CdS<CdSe<ZnS.

That is, the introduction of a CdS layer between TiO_2 and CdSe elevates the conduction band edge of CdSe, giving a higher driving force for the injection of excited electrons out of the CdSe layer (Kim et al.., 2009). Second, the photocurrent density might be enhanced with QDs loading by means of increasing coating cycles (Chris et al.., 2003).

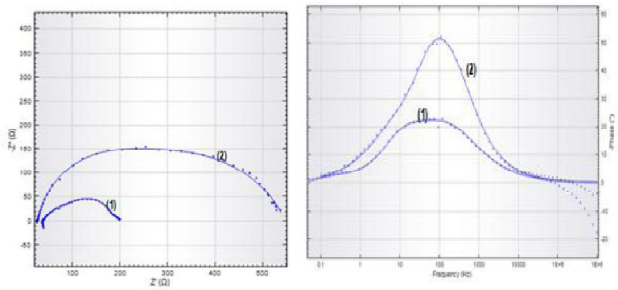

Figure 6. (a) Nyquist plots of TiO_2/CdS(3)/CdSe(3)/ZnS(2) QDSSCs and (b) Bode curves.

In order to reveal the micro mechanism of the QDSSCs, EIS has been carried out under dark conditions at varying negative applied bias (0.7 V–0 V). Figure 6 shows the Nyquist plots of the CdS (3)/CdSe (3)/ZnS (2) QDs - sensitized solar cells. We find two semicircle of the EIS spectra at high frequency and low frequency. The small semicircle at high frequency corresponds to the resistance movement of particles at interface of counter electrode/electrolyte (R_{ct1}) and FTO/TiO_2 interface. The large semicircle at low frequency from 10-100 kHz described resistance against the movement of electron in the semiconductor TiO_2 and the charge recombination resistance at the TiO_2/QDs/electrolyte interface (R_{ct2}) and against inside the diffusion in of electrolyte (Z_w).

From Figure 6a, we see that the R_{ct2}value obtainedabout520Ω when annealing was 150^{o}C. The resistance of R_{ct2}decreased down to 200Ω when annealing was 300^{o}C correspond to the narrowed semicircle. it mean that resistance the movement of electrons at the interface of TiO_2/QDs/electrolyte and recombination of the electrons and polysulfide increased when annealing decreased (Balisa et al.., 2013). The reason mean that the crystallized QDs at 300^{o}C is better than its at 150^{o}C.At 300^{o}C, the crystallization of QDs become perfect, so recombination process reduced in semiconductor.

Figure 6b shows the Bode plot of the QDSSCs with TiO_2/CdS(3)/CdSe(3)/ZnS(2) photo anode that is illuminated with an 1000W/m^2. At low frequency peaks corresponds to the movement of electrons at the interface TiO_2/QDs/electrolyte, while the peak at higher frequencies to describe the movement of the particles at the interface Pt/electrolyte. Lifetime of electrons in semiconductor (τ_e) is determined by the following formula = $1/2\pi f_{max}$. The f_{max} is the peak of the Bode plot at low frequencies, τ_e~1.77ms.The results show that Bode plots shifted toward the low frequency as annealing at 300^{o}C corresponding to the increased lifetime of electrons. Results of Bode plots agree good with Nyquist's.

IV. CONCLUSIONS

We successfully conducted quantum dots solar cells based on set of the CdS/CdSe/ZnS photo anodes by successive ionic layer absorption and reaction (SILAR) processes. The results show that the open circuit increased from 0.29 V to 0.79 V because the stimulated electrons were efficiently generated in the conduction band of quantum dots when the number SILAR changed. Moreover, The resistance of R_{ct2} decreased down to 200 Ω when annealing was 300^{o}C correspond to the narrowed semicircle and Bode plots shifted toward the low frequency as annealing at 300^{o}C corresponding to the increased lifetime of electrons. The synthesized TiO_2/CdS/CdSe/ZnS photo anode obtained a high maximum efficiency of 1.52%.

REFERENCES

[1] Grätzel M. Photoelectrochemical cells. Nature. 2001; 414.6861: 338-344

[2] Wijayantha KGU, Peter LM, Otley LC. Sol. Fabrication of US quantum dot sensitized solar cells via a pressing route. Energy Mater. Sol. Cells. 2004; 83,363.

[3] Padinger F, Rittberger RS, Sariciftci NS.Low-Cost Nanomaterials.Adv. Funct. Mater. 2009;19, 2735.

[4] Tubtimtae A, Wu KL, Tung HY, Lee MW, Wang GJ.Ag2S quantum dot-sensitized solar cells. Electrochem. Commun. 2010;12, 1158.

[5] Fuke N, Hoch LB, Koposov AY, Manner VW, Werder DJ, Fukui A, Koide N, Katayama H, Sykora M.CdSe Quantum-Dot-Sensitized Solar Cell with ~100% Internal Quantum Efficiency. ACS Nano.2007; 4, 6377.

[6] Tubtimtae A, Lee MW, Wang GJ. Ag2Se quantum-dot sensitized solar cells for full solar spectrum light harvesting.J. Power Sources. 2011; 196, 6603.

[7] Bang JH, Kamat PV.Tailored TiO2−SrTiO3 heterostructure nanotube arrays for improved photoelectrochemical performance. ACS Nano.2009; 3,1467.

[8] Yu PR, Zhu K, Norman AG, Ferrere S, Frank AJ, Nozik AJ.Multiexciton generation by a single photon in Nanocrystalline TiO2 solar cells.J. Phys. Chem. B. 2006; 110, 25451.

[9] Gorer S, Hodes G. Solution Deposition of Semiconductor Films.J. Phys. Chem. 1994;98, 5338.

[10] Moreels I, Lambert K, De D,Muynck F,Vanhaecke D,Poelman JC. Martins, G. Allan, Z. Hens.Composition and size-dependent extinction coefficient of colloidal PbSe quantum dots. Chem. Mater. 2007;19, 6101.

[11] Nozik AJ.Physical chemistry of semiconductor-liquid interfaces.J. Chem. Phys. Lett.2008; 457,3.

[12] Hanna MC, Nozic AJJ. J. Appl. Phys. 2006; 100, 074510.

[13] Lee YL, Lo YS.Highly efficient quantum-dot-sensitized solar cell based on Co-sensitization of CdS/CdSe. Adv. Funct. Mater. 2009;19, 604

[14] Gonzalez-Pedro V, Xu X, Mora-Sero I, Bisquert J. Modeling high-efficiency quantum dot sensitized solar cells. ACS Nano. 2010; 4:5783–90.

[15] Pathan HM, Lokhande CD.Deposition of metal chalcogenide thin films by successive ionic layer adsorption and reaction (SILAR) method. Bulletin of Materials Science 27. 2004; 2: 85-111.

[16] Tachan Z, Shalom M, Hod I, Ruhle S, Tirosh S, Zaban A. J. Phys. Chem. C. 2011; 115, 6162.

[17] Lee YL, Lo YS. Highly efficient quantum-dot-sensitized solar cell based on co-sensitization of CdS/CdSe. Advanced Functional Materials. 2009; 9:604–9.

[18] Kim JK, Choi SH, Noh JH, Yoon SH, Lee SW, Noh TH, Frank AJ, Hong KS.Synthesis, characterization, and comparative study of

CdSe–TiO2 nanowires and CdSe–TiO2 nanoparticles.Langmuir. 2009; 25, 5348.

[19] Sudhagar P, Jung JH, Park S, Lee YG, Sathyamoorthy R, Kang YS, Ah H. The performance of coupled (CdS:CdSe) quantum dot-sensitized TiO2nanofibrous solar cells. Electrochemistry Communications. 2009; 11 2220–2224.

[20] Balisa N, Dracopoulosb V, Bourikasc K, Lianos P. Quantum dot sensitized solar cells based on an optimized combination of ZnS, CdS and CdSe with CoS and CuS counter electrodes. ElectrochimicaActa. 2013; 91, 246–252.

[21] Chris GV, Neugebauer J. Nature.2003; 423, 626.